PHYSICAL REVIEW C **88**, 051302(R) (2013)

Quadrupole-octupole coupling in the light actinides

L. M. Robledo[1,*] and P. A. Butler[2]
[1]*Departamento de Física Teórica, Universidad Autónoma de Madrid, E-28049 Madrid, Spain*
[2]*Oliver Lodge Laboratory, University of Liverpool, Liverpool L69 7ZE, United Kingdom*
(Received 20 September 2013; published 11 November 2013)

The relevance of coupling of quadrupole and octupole collective degrees of freedom in physical observables is explored in calculations with the Gogny force for the light radon, radium, and thorium isotopes. The results of the generator coordinate method calculations for the properties of negative parity states show an improvement over the traditional ones that consider just the octupole moment.

DOI: 10.1103/PhysRevC.88.051302 PACS number(s): 21.10.Re, 21.60.Ev, 21.60.Fw, 21.60.Jz

Introduction. Permanent octupole deformed shapes, predicted long ago to be present in the intrinsic ground state of several light actinides [1], can be inferred by combining the two signatures of octupole deformation, namely, low-lying negative parity states and strong $E3$ strengths. Information on $E3$ strengths in this mass region has recently been extended by Coulomb excitation measurements of ^{220}Rn and ^{224}Ra [2]. These results can be nicely understood from a theoretical perspective by using sound theoretical methods including parity projection and configuration mixing based on Hartree-Fock-Bogoliubov wave functions [3,4] and the Gogny class of energy density functionals [5]. It turns out that the intrinsic states showing octupole deformation in the light actinides also have quadrupole deformation with the deformation parameter β_2 in the range 0.05–0.25 which is a small value for a well deformed nucleus. According to the accumulated theoretical knowledge, small ground state β_2 values at the mean field level usually entail a relevant role of quantum fluctuations. The impact of them on nuclear properties can eventually wash out the original mean field description. In those cases, it is advisable to explore the quadrupole degree of freedom in a framework where its quantum fluctuations can be properly addressed: the generator coordinate method (GCM) [3]. The purpose of this paper is to present the results obtained for the low energy dynamics of several light actinides by exploring the axially symmetric quadrupole and octupole degrees of freedom in a mean field framework including configuration mixing and using the well known and reputed Gogny functionals. The two parametrizations considered, D1S [6] and D1M [7], have been applied before to describe octupole properties in a variety of cases [4,8–11]. On the other hand, the quadrupole-octupole coupling with Skyrme or Gogny forces has been treated before in a similar framework [9,12–14]. Our study includes results for the even-even isotopes of radon, radium, and thorium with neutron numbers in the range $N = 130$–142. The evolution with mass number of several observables, like the excitation energies of 1^- and 3^- states, the dipole $E1$ and octupole $E3$ transition strengths as well as properties of the quadrupole vibrational states are discussed and compared to experimental data.

Methods. The starting point for the theoretical description of the quadrupole-octupole dynamics is the mean field Hartree-Fock-Bogoliubov (HFB) method [3] with the Gogny energy density functional (EDF) [5]. Two parametrizations of the Gogny EDF will be considered: the more traditional D1S parametrization [6] that has been tested in a variety of different physical scenarios, and the recently proposed D1M parametrization [7] aimed at improving the poor performance of D1S in describing nuclear masses. An important simplification of the model is the restriction to axially symmetric shapes that limit the number of relevant degrees of freedom to just two: the ones corresponding to the $K = 0$ component of the quadrupole Q_{20} and octupole Q_{30} operators. A set of HFB wave functions $|\phi(Q_{20}, Q_{30})\rangle$ is obtained by solving the constrained HFB equation for different values of Q_{20}-Q_{30} in a mesh with $N_2 = 50$ ($N_3 = 29$) points along the Q_{20} (Q_{30}) directions and the ranges $Q_{20} \in [-20\ \mathrm{b}, 30\ \mathrm{b}]$ and $Q_{30} \in [-7.5\ \mathrm{b}^{3/2}, 7.5\ \mathrm{b}^{3/2}]$ (wave functions with negative Q_{30} values are obtained from the positive Q_{30} ones by application of the parity operator). As the number of HFB configurations involved is large $[N_2(N_3 + 1)/2 = 750]$, a well performing and robust algorithm to solve the HFB equation is required. We have used the approximate second-order gradient method described in [15] and implemented in the HFBAXIAL code developed by one of the authors [16]. The intrinsic and correlated wave functions $|\Psi_\sigma\rangle$ of the generator coordinate method [3] kind are linear combinations of the HFB states

$$|\Psi_\sigma\rangle = \iint dQ_{20} dQ_{30} f_\sigma(Q_{20}, Q_{30}) |\phi(Q_{20}, Q_{30})\rangle.$$

The GCM amplitudes $f_\sigma(Q_{20}, Q_{30})$ are the solution of the Hill-Wheeler (HW) equation which is the Schrödinger equation in the subspace spanned by the HFB states $|\phi(Q_{20}, Q_{30})\rangle$. Along with the GCM amplitudes, the HW equation also provides the energies E_σ of each correlated state σ. As the parity operator reverses the sign of Q_{30} in the HFB states, the parity π_σ of $|\Psi_\sigma\rangle$ is determined by the one in $f_\sigma(Q_{20}, -Q_{30}) = \pi_\sigma f_\sigma(Q_{20}, Q_{30})$. Mean values and overlaps of observables are computed following the rules of quantum mechanics

$$\langle \Psi_\sigma | \hat{O} | \Psi_{\sigma'} \rangle = \iint d\mathbf{Q} d\mathbf{Q}'\ f^*_\sigma(\mathbf{Q}) f_{\sigma'}(\mathbf{Q}') \langle \phi(\mathbf{Q}) | \hat{O} | \phi(\mathbf{Q}') \rangle.$$

*luis.robledo@uam.es; http://gamma.ft.uam.es/robledo

Overlaps are required in the evaluation of electromagnetic transition strengths, where the validity of the rotational formula is assumed for strongly quadrupole deformed states. For instance, if $|\Psi_0\rangle$ and $|\Psi_1\rangle$ are the intrinsic states corresponding to the 0^+ and 3^- physical states, the $E3$ transition strength is given by

$$B(E3, 3^- \to 0^+) = e^2/(4\pi)|\langle\Psi_0|\hat{Q}_{30}|\Psi_1\rangle|^2.$$

As discussed in [17] the use of the rotational formula to obtain transition strengths is not well justified in weakly deformed systems like some of the lighter Rn and Ra isotopes considered here. The main conclusion of the study is that the use of angular momentum projected wave functions in the calculation of the transition strengths for near spherical systems leads to increases in the $B(E3)$ strengths as large as a factor of 7 with respect to the rotational formula results. For correlated GCM wave functions the situation is more complex as it requires transition strengths between different intrinsic states that are subsequently weighted by the collective amplitudes. As no general conclusions can be extracted in this case, the use of the fully-fledged projected calculations is recommended. However, the large number of configurations to consider render the calculations computationally expensive. Exploratory results indicate that the projected strengths get in fact reduced in all the cases (probably as a consequence of configuration mixing) by around 10%. More on this issue will be presented elsewhere.

In the discussion of the results below the probability amplitudes of the correlated states $|\Psi_\sigma\rangle$ will be required. The $f_\sigma(\mathbf{Q})$ amplitudes are not the proper quantities because they are associated with a non-orthogonal basis where the norm overlap $\mathcal{N}(\mathbf{Q}, \mathbf{Q}') = \langle\phi(\mathbf{Q})|\phi(\mathbf{Q}')\rangle$ is not a δ function. Instead, one has to consider the amplitudes

$$g_\sigma(\mathbf{Q}) = \int d\mathbf{Q}'\, \mathcal{N}^{1/2}(\mathbf{Q}, \mathbf{Q}')\, f_\sigma(\mathbf{Q}'),$$

which are the real probability amplitudes for the configuration with deformation $\mathbf{Q}$.

The evaluation of the Hamiltonian overlaps that enter the HW equation pose a problem when density dependent interactions are considered. A prescription is used to compute those overlaps that is at the same time consistent [18] with the underlying mean field and free from pathology [19].

Results. Calculations along the line described above have been carried out for the even-even isotopes of Rn, Ra, and Th species with neutron numbers in the range between $N = 130$ and $N = 142$. Two sets of calculations with Gogny D1S and D1M have been considered in order to assess the uncertainties in the predictions with respect to the details of the interaction. Previous calculations in the context of the collective Schrödinger equation (an approximation to the full GCM) were reported in the past [9]. In Fig. 1 the HFB energies $E(Q_{20}, Q_{30})$ and the collective amplitudes $|g_\sigma(Q_{20}, Q_{30})|^2$ for the ground state and the first negative parity excited state are plotted for four representative nuclei: ^{220}Rn, ^{224}Ra, ^{228}Th, and ^{232}Th. The nucleus ^{220}Rn is a typical example of a weakly deformed quadrupole and octupole nucleus with a HFB energy which is soft along the quadrupole and octupole directions. The ^{224}Ra isotope is another typical example of a weakly deformed quadrupole nucleus but with a well developed octupole deformed minimum. The isotope ^{228}Th is well deformed in the quadrupole degree of freedom and weakly octupole deformed. Finally, ^{232}Th is an example of a well deformed nucleus which is reflection symmetric and very stiff along the quadrupole direction. The energies have a parabolic behavior around the

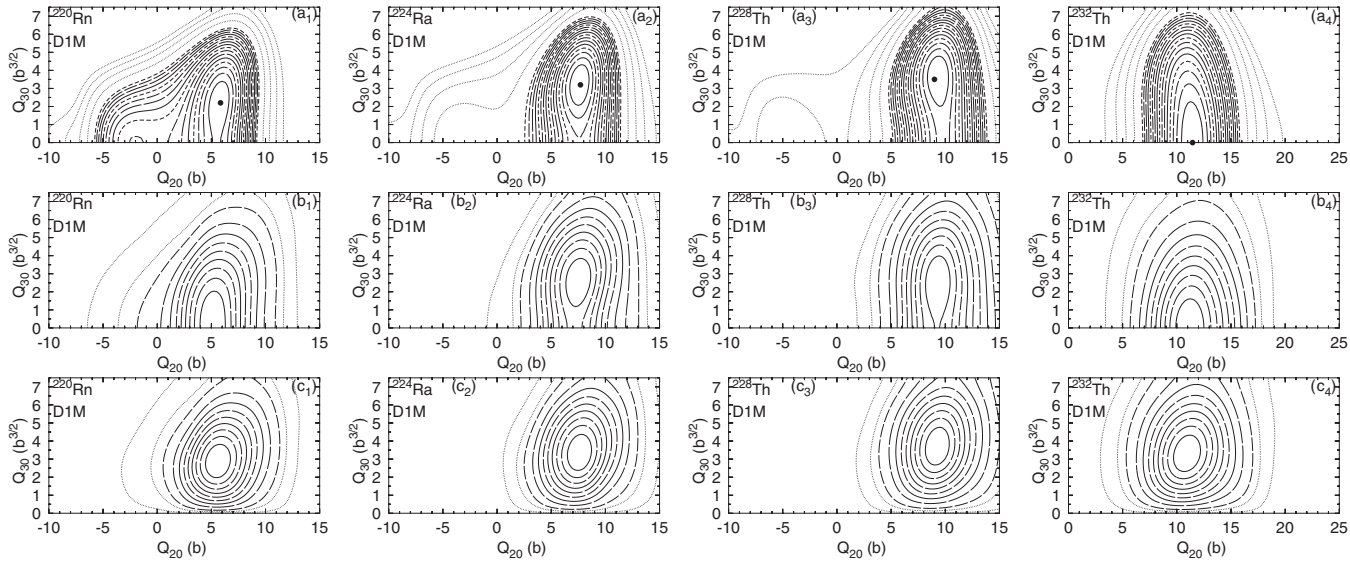

FIG. 1. Upper row (a_1 to a_4): contour plots of the HFB energy surfaces $E(Q_{20}, Q_{30})$ obtained with the Gogny D1M interaction are depicted for several nuclei considered in this work. The position of the ground state minimum is signalled by a bullet. In the middle row (b_1 to b_4) the ground state collective amplitudes $|g_\sigma(Q_{20}, Q_{30})|^2$ are shown. In the bottom row (c_1 to c_4), the corresponding amplitudes for the first negative parity excited state are given. In this mass region a Q_{20}value of 1b corresponds to a $\beta_2 = 0.022$ and a Q_{30} of 1 $b^{3/2}$ to $\beta_3 = 0.035$. All quantities are symmetric under the $Q_{30} \to -Q_{30}$ exchange. For the HFB energies, contour lines (full and dashed) are plotted every 250 keV up to 4 MeV and from there on (dotted) every 1 MeV up to 8 MeV.

minimum which is not easy to reconcile with some recent models of quadrupole-octupole coupling [22] that require potential energies resembling an infinite depth square well potential. The ground state collective amplitudes obtained in the GCM calculation are shown in the middle row of Fig. 1. They follow closely the shape of the HFB energy with maxima correlated with the positions of the HFB energy minima. They look like two-dimensional Gaussian functions centered at the position of the HFB minima. Finally, the collective amplitudes of the first negative parity state are presented in the bottom row. Their shapes are rather similar to the ones of the ground state except for the symmetry requirement that the collective amplitude is zero along the $Q_{30} = 0$ line. It favors the shifting of the maxima to Q_{30} values larger than the ones observed in the ground state amplitudes. Only in the ^{224}Ra case, and to a lesser extent in ^{228}Th, both the ground state and first negative parity state amplitudes have a large overlap, favoring a small energy splitting and strong $E3$ transition probabilities, typical signatures of octupole deformed systems.

The concept of quantum phase transitions (QPTs) is often called for to interpret the behavior of physical observables in isotopic or isotonic chains. In the octupole case, it is argued that those nuclei with a well deformed octupole minimum could signal the transition point of such a QPT as a function of neutron number, and the example of ^{226}Th is often mentioned in the literature. Although the results of Fig. 1 do not include the whole thorium chain, its main features can be discussed because ^{224}Th and ^{226}Th both look rather similar to ^{224}Ra. From the figure we conclude that the three quantities, HFB energies, and the collective amplitudes $|g_\sigma(Q_{20}, Q_{30})|^2$ for the ground and first negative parity states, behave smoothly as a function of neutron number for the Th isotopes. As the collective amplitudes determine the final values and evolution of the physical observables, see below, we conclude that no discontinuities are expected in the thorium chain (see below), as it would be required by a QPT.

The physical quantities obtained in the GCM calculations are the intrinsic energy of the lowest lying negative parity state, various mean values of operators and transition strengths. As typical moments of inertia are rather large in the region, the rotational energy associated with the physical 1^- and 3^- states is much smaller than the splitting with the ground state and will not be considered explicitly here. In Fig. 2 the results for the 1^- excitation energy and $B(E1)$ and $B(E3)$ transition strengths to the ground state (in Weisskopf units) are given for the three isotopic chains considered. Both the results of the two-dimensional calculation Q_{20}-Q_{30} and the one-dimensional one of [4] are presented for comparison. The consequences of

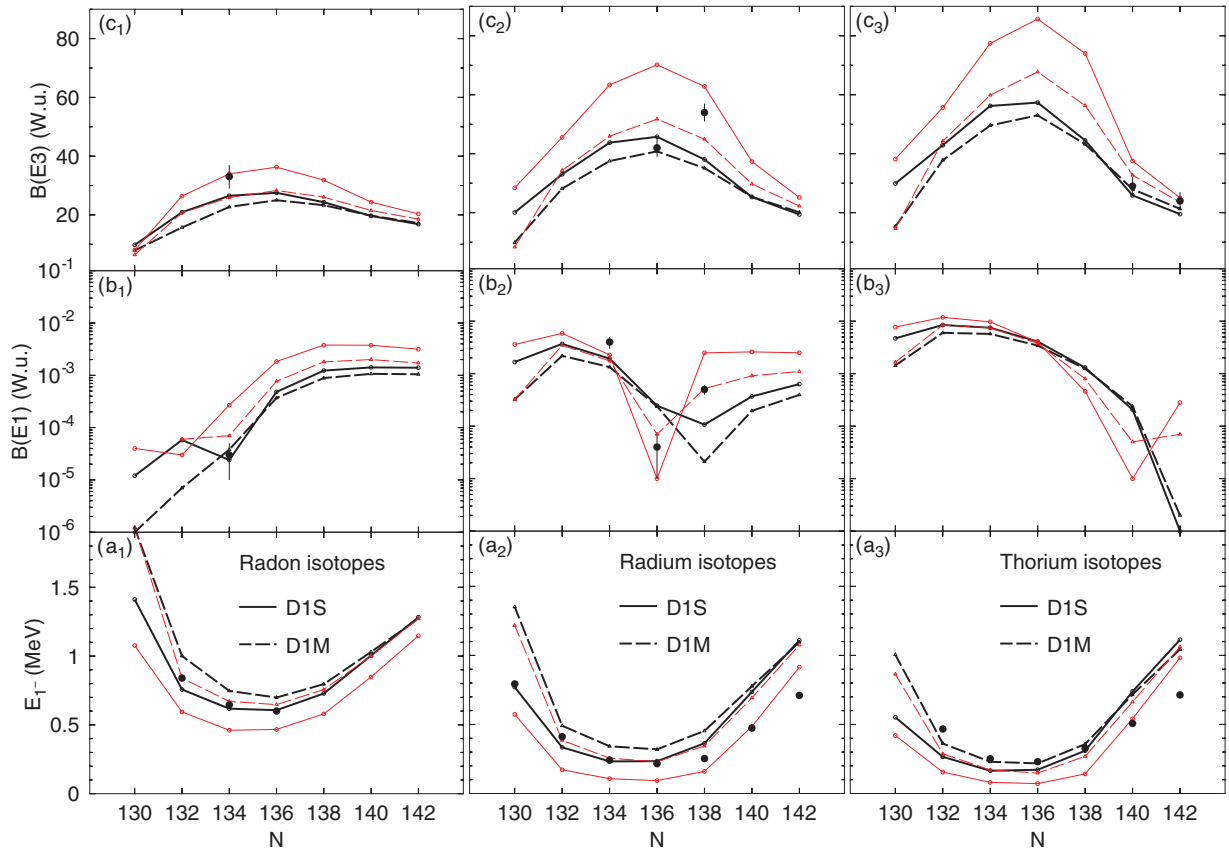

FIG. 2. (Color online) Excitation energies of the 1^- state (panels a_1 to a_3) and transition strengths to the ground state $B(E1)$ (panels b_1 to b_3) and $B(E3)$ (panels c_1 to c_3) (in Weisskopf units) are depicted for the radon, radium, and thorium isotopic chains. Experimental results are represented by bullets whereas the theoretical predictions obtained with the two-dimensional Q_{20}-Q_{30} GCM calculations are plotted as full (dotted) black lines for Gogny D1S (D1M). Results of the one-dimensional GCM calculation with Q_{30} as collective coordinate are represented by red (gray) lines. Experimental results are from [2] for ^{220}Rn and ^{224}Ra and from other sources [20,21] for the other nuclei.

including the coupling to the quadrupole degree of freedom are an increase of the 1^- excitation energy and a decrease of the $B(E3)$ transition strength from the 3^- to the 0^+. Both effects are characteristic of a quenching of octupole correlations. For $B(E1)$ the impact is more nucleus dependent as a consequence of the much less collective character of the dipole operator (see [11] for a recent discussion). In fact, the minimum observed at $N = 134$ for $B(E1)$ in the one-dimensional calculation of [4] is shifted to $N = 136$, worsening the agreement with experiment. It is also a systematic effect that the D1S and D1M results in the Q_{20}-Q_{30} calculation are much closer to each other than in the calculation with Q_{30} alone. The comparison with experiment is rather satisfactory as both excitation energies and transition strengths are well reproduced. Perhaps the theoretical excitation energies are a bit too high for the heavier isotopes but this seems to be a common deficiency of GCM calculations [4,23] for vibrational-like states.

The proton-neutron interaction [24] is often invoked in order to understand structural changes along isotopic chains [25,26]. For instance, the binding energy filter

$$V_{pn}(Z,N) = \tfrac{1}{4}[B(Z,N) - B(Z-2,N) - B(Z,N-2) + B(Z-2,N-2)]$$

has been used to signal the transition to an octupole deformation regime in the ground state as well as the relevance of additional quantum correlations [27,28]. To test this concept we have represented this quantity in Fig. 3 as a function of neutron number N. Only the results with D1M are presented because D1S is well known to poorly reproduce binding energies. For both Ra and Th we observe a large discrepancy with experiment at $N = 132$, which corresponds to octupole deformed nuclei but with very swallow minima. The addition of correlations improve the agreement with experiment. The Ra isotopes with $N = 138$ and 140 show large discrepancies between the mean field results (both reflection symmetric and asymmetric) and the experiment. Again, considering correlations improves the agreement substantially. These nuclei are octupole deformed but with potential wells not well developed. A similar situation is observed for the Th isotopes with neutron

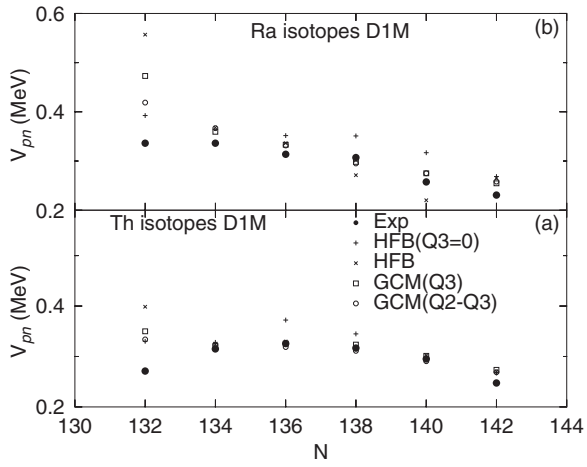

FIG. 3. The proton-neutron energy V_{pn} defined in the text is plotted as a function of neutron number N for the radium (b) and thorium (a) isotopes.

TABLE I. Comparison between experimental [2] and theoretical values of different physical observables.

	^{220}Rn		^{224}Ra	
	Q_{20}-Q_{30}	Expt.	Q_{20}-Q_{30}	Expt.
E_{1^-} (MeV)	0.618	0.645	0.234	0.216
$B(E1)$ (Wu)	2.4×10^{-5}	$<1.5 \times 10^{-3}$	2.4×10^{-4}	$<5 \times 10^{-5}$
$B(E3)$ (Wu)	26.50	33 ± 4	45.74	42 ± 3
E_{2^+} (Vib)	1.860	0.938	1.746	0.966
$B(E2)$ (Wu)	48.47	48 ± 3	92.75	98 ± 3

numbers $N = 136$ and 138. Here, contrary to the Ra case, the octupole deformed HFB calculation already provides good agreement with experiment and this is only improved slightly by the inclusion of correlations. A discrepancy between experiment and theory in V_{pn}, like the one at $N = 132$, signals that some physics is missing, but we cannot conclude from that discrepancy alone whether it is a mean field effect (breaking of symmetries) or a quantum correlation effect.

Another relevant piece of experimental information obtained in [2] is the excitation energy of the vibrational 2^+ state and the $B(E2)$ transition strength from the 2^+ member of the ground state rotational band to the ground state. The experimental results for ^{220}Rn and ^{224}Ra are compared in Table I with the theoretical results obtained with Gogny D1M (the results with D1S are similar). We observe a good agreement between calculations and experimental data except for the excitation energy of the β vibration that comes out a factor of 2 larger. This is a well known problem in the theoretical description of the β vibrations. However, for ^{224}Ra, the inclusion of the quadrupole-octupole coupling improves the description of this state as compared with that obtained using a one-dimensional GCM calculation with only the quadrupole degree of freedom. We go from the 2.45 MeV obtained in the one-dimensional case to the 1.75 MeV shown in the table, showing the relevance of the quadrupole-octupole coupling in the description of this observable.

Conclusions. We have analyzed the onset of octupole collectivity in several isotopes of Rn, Ra, and Th using advanced models of nuclear structure. A two-dimensional GCM calculation to deal with the quadrupole-octupole coupling and using two variants of the Gogny force is performed for each isotope. The results for excitation energies and transition strengths agree quite well with recent experimental findings. The impact of correlations on the behavior of the proton-neutron interaction as a function of neutron number is found to be small but it always goes in the direction of improving the agreement with experiment. The potential energy surfaces show a parabolic behavior around the minimum that differs from commonly used ones in simple models of quadrupole-octupole coupling. The behavior of physical quantities and probability amplitudes do not show any of the abrupt discontinuities which are characteristic of QPT.

Acknowledgments. The work of L.M.R. is supported in part by MICINN Grants No. FPA2012-34694 and No. FIS2012-34479 and by the Consolider-Ingenio 2010 program MULTIDARK CSD2009-00064. P.A.B. acknowledges support from the UK STFC.

[1] P. A. Butler and W. Nazarewicz, Rev. Mod. Phys. **68**, 349 (1996).
[2] L. P. Gaffney *et al*., Nature **497**, 199 (2013).
[3] P. Ring and P. Schuck, *The Nuclear Many-Body Problem* (Springer, New York, 1980).
[4] L. M. Robledo and G. F. Bertsch, Phys. Rev. C **84**, 054302 (2011).
[5] J. Decharge and D. Gogny, Phys. Rev. C **21**, 1568 (1980).
[6] J. F. Berger, M. Girod, and D. Gogny, Nucl. Phys. A **428**, 23c (1984).
[7] S. Goriely, S. Hilaire, M. Girod, and S. Perú, Phys. Rev. Lett. **102**, 242501 (2009).
[8] E. Garrote, J. L. Egido, and L. M. Robledo, Phys. Rev. Lett. **80**, 4398 (1998).
[9] L. M. Robledo, J. L. Egido, B. Nerlo-Pomorska, and K. Pomorski, Phys. Lett. B **201**, 409 (1988).
[10] R. Rodriguez-Guzman, L. M. Robledo, and P. Sarriguren, Phys. Rev. C **86**, 034336 (2012).
[11] L. M. Robledo and R. R. Rodriguez-Guzman, J. Phys. G **39**, 105103 (2012).
[12] J. Skalski, P.-H. Heenen, and P. Bonche, Nucl. Phys. A **559**, 221 (1993).
[13] P. Bonche, P. H. Heenen, H. Flocard, and D. Vautherin, Phys. Lett. B **175**, 387 (1986).
[14] J. Meyer, P. Bonche, MS Weiss, J. Dobaczewski, H. Flocard, and P.-H. Heenen, Nucl. Phys. A **588**, 597 (1995).
[15] L. M. Robledo and G. F. Bertsch, Phys. Rev. C **84**, 014312 (2011).
[16] L. M. Robledo, HFBAXIAL code (2002).
[17] L. M. Robledo and G. F. Bertsch, Phys. Rev. C **86**, 054306 (2012).
[18] L. M. Robledo, Intl. J. Mod. Phys. E **16**, 337 (2007).
[19] L. M. Robledo, J. Phys. G **37**, 064020 (2010).
[20] H. J. Wollersheim *et al*., Nucl. Phys. A **556**, 261 (1993).
[21] T. Kibédi and R. Spear, At. Data Nucl. Data Tables **80**, 35 (2002).
[22] P. G. Bizzeti and A. M. Bizzeti-Sona, Phys. Rev. C **88**, 011305(R) (2013).
[23] S. Péru, J. F. Berger, and P. F. Bortignon, Eur. Phys. J. A **26**, 25 (2005).
[24] I. Talmi, Rev. Mod. Phys. **34**, 704 (1962); P. Federman and S. Pittel, Phys. Lett. B **69**, 385 (1977).
[25] R. B. Cakirli, D. S. Brenner, R. F. Casten, and E. A. Millman, Phys. Rev. Lett. **94**, 092501 (2005).
[26] M. Stoitsov, R. B. Cakirli, R. F. Casten, W. Nazarewicz, and W. Satula, Phys. Rev. Lett. **98**, 132502 (2007).
[27] L. F. Yu, P. W. Zhao, S. Q. Zhang, and J. Meng, arXiv:1211.0601.
[28] E. Olsen, J. Erler, W. Nazarewicz, and M. Stoitsov, J. Phys.: Conf. Ser. **402**, 012034 (2012).